Hindawi Publishing Corporation
Mathematical Problems in Engineering
Volume 2012, Article ID 405870, 22 pages
doi:10.1155/2012/405870

Research Article

The Orbital Dynamics of Synchronous Satellites: Irregular Motions in the 2 : 1 Resonance

Jarbas Cordeiro Sampaio,[1] Rodolpho Vilhena de Moraes,[2] and Sandro da Silva Fernandes[3]

[1] *Departamento de Matemática, Universidade Estadual Paulista (UNESP), 12516-410 Guaratinguetá-SP, Brazil*
[2] *Instituto de Ciência e Tecnologia, Universidade Federal de São Paulo (UNIFESP), 12231-280 São José dos Campos, SP, Brazil*
[3] *Departamento de Matemática, Instituto Tecnológico de Aeronáutica (ITA), 12228-900 São José dos Campos, SP, Brazil*

Correspondence should be addressed to Jarbas Cordeiro Sampaio, jarbascordeiro@gmail.com

Received 7 July 2011; Accepted 27 September 2011

Academic Editor: Silvia Maria Giuliatti Winter

The orbital dynamics of synchronous satellites is studied. The 2 : 1 resonance is considered; in other words, the satellite completes two revolutions while the Earth completes one. In the development of the geopotential, the zonal harmonics J_{20} and J_{40} and the tesseral harmonics J_{22} and J_{42} are considered. The order of the dynamical system is reduced through successive Mathieu transformations, and the final system is solved by numerical integration. The Lyapunov exponents are used as tool to analyze the chaotic orbits.

1. Introduction

Synchronous satellites in circular or elliptical orbits have been extensively used for navigation, communication, and military missions. This fact justifies the great attention that has been given in literature to the study of resonant orbits characterizing the dynamics of these satellites since the 60s [1–14]. For example, Molniya series satellites used by the old Soviet Union for communication form a constellation of satellites, launched since 1965, which have highly eccentric orbits with periods of 12 hours. Another example of missions that use eccentric, inclined, and synchronous orbits includes satellites to investigate the solar magnetosphere, launched in the 90s [15].

The dynamics of synchronous satellites are very complex. The tesseral harmonics of the geopotential produce multiple resonances which interact resulting significantly in nonlinear motions, when compared to nonresonant orbits. It has been found that the orbital

elements show relatively large oscillation amplitudes differing from neighboring trajectories [11].

Due to the perturbations of Earth gravitational potential, the frequencies of the longitude of ascending node Ω and of the argument of pericentre ω can make the presence of small divisors, arising in the integration of equation of motion, more pronounced. This phenomenon depends also on the eccentricity and inclination of the orbit plane. The importance of the node and the pericentre frequencies is smaller when compared to the mean anomaly and Greenwich sidereal time. However, they also have their contribution in the resonance effect. The coefficients l, m, p which define the argument ϕ_{lmpq} in the development of the geopotential can vary, producing different frequencies within the resonant cosines for the same resonance. These frequencies are slightly different, with small variations around the considered commensurability.

In this paper, the $2:1$ resonance is considered; in other words, the satellite completes two revolutions while the Earth carries one. In the development of the geopotential, the zonal harmonics J_{20} and J_{40} and the tesseral harmonics J_{22} and J_{42} are considered. The order of the dynamical system is reduced through successive Mathieu transformations, and the final system is solved by numerical integration. In the reduced dynamical model, three critical angles, associated to the tesseral harmonics J_{22} and J_{42}, are studied together. Numerical results show the time behavior of the semimajor axis, argument of pericentre and of the eccentricity. The Lyapunov exponents are used as tool to analyze the chaotic orbits.

2. Resonant Hamiltonian and Equations of Motion

In this section, a Hamiltonian describing the resonant problem is derived through successive Mathieu transformations.

Consider (2.1) to the Earth gravitational potential written in classical orbital elements [16, 17]

$$V = \frac{\mu}{2a} + \sum_{l=2}^{\infty} \sum_{m=0}^{l} \sum_{p=0}^{l} \sum_{q=+\infty}^{-\infty} \frac{\mu}{a} \left(\frac{a_e}{a}\right)^l J_{lm} F_{lm}(I) G_{lpq}(e) \cos\left(\phi_{lmpq}(M, \omega, \Omega, \theta)\right), \tag{2.1}$$

where μ is the Earth gravitational parameter, $\mu = 3.986009 \times 10^{14}\,\mathrm{m}^3/\mathrm{s}^2$, a, e, I, Ω, ω, M are the classical keplerian elements: a is the semimajor axis, e is the eccentricity, I is the inclination of the orbit plane with the equator, Ω is the longitude of the ascending node, ω is the argument of pericentre, and M is the mean anomaly, respectively; a_e is the Earth mean equatorial radius, $a_e = 6378.140\,\mathrm{km}$, J_{lm} is the spherical harmonic coefficient of degree l and order m, $F_{lmp}(I)$ and $G_{lpq}(e)$ are Kaula's inclination and eccentricity functions, respectively. The argument $\phi_{lmpq}(M, \omega, \Omega, \theta)$ is defined by

$$\phi_{lmpq}(M, \omega, \Omega, \theta) = qM + (l - 2p)\omega + m(\Omega - \theta - \lambda_{lm}) + (l - m)\frac{\pi}{2}, \tag{2.2}$$

where θ is the Greenwich sidereal time, $\theta = \omega_e t$ (ω_e is the Earth's angular velocity, and t is the time), and λ_{lm} is the corresponding reference longitude along the equator.

In order to describe the problem in Hamiltonian form, Delaunay canonical variables are introduced,

$$L = \sqrt{\mu a}, \qquad G = \sqrt{\mu a(1-e^2)}, \qquad H = \sqrt{\mu a(1-e^2)}\cos(I),$$
$$\ell = M, \qquad g = \omega, \qquad h = \Omega. \tag{2.3}$$

L, G, and H represent the generalized coordinates, and ℓ, g, and h represent the conjugate momenta.

Using the canonical variables, one gets the Hamiltonian $\widehat{F}$,

$$\widehat{F} = \frac{\mu^2}{2L^2} + \sum_{l=2}^{\infty}\sum_{m=0}^{l} R_{lm}, \tag{2.4}$$

with the disturbing potential R_{lm} given by

$$R_{lm} = \sum_{p=0}^{l}\sum_{q=-\infty}^{+\infty} B_{lmpq}(L,G,H)\cos\left(\phi_{lmpq}(\ell,g,h,\theta)\right). \tag{2.5}$$

The argument ϕ_{lmpq} is defined by

$$\phi_{lmpq}(\ell,g,h,\theta) = q\ell + (l-2p)g + m(h-\theta-\lambda_{lm}) + (l-m)\frac{\pi}{2}, \tag{2.6}$$

and the coefficient $B_{lmpq}(L,G,H)$ is defined by

$$B_{lmpq} = \sum_{l=2}^{\infty}\sum_{m=0}^{l}\sum_{p=0}^{l}\sum_{q=+\infty}^{-\infty}\frac{\mu^2}{L^2}\left(\frac{\mu a_e}{L^2}\right)^l J_{lm}F_{lmp}(L,G,H)G_{lpq}(L,G). \tag{2.7}$$

The Hamiltonian $\widehat{F}$ depends explicitly on the time through the Greenwich sidereal time θ. A new term $\omega_e\Theta$ is introduced in order to extend the phase space. In the extended phase space, the extended Hamiltonian $\widehat{H}$ is given by

$$\widehat{H} = \widehat{F} - \omega_e\Theta. \tag{2.8}$$

For resonant orbits, it is convenient to use a new set of canonical variables. Consider the canonical transformation of variables defined by the following relations:

$$X = L, \qquad Y = G - L, \qquad Z = H - G, \qquad \Theta = \Theta,$$
$$x = \ell + g + h, \qquad y = g + h, \qquad z = h, \qquad \theta = \theta, \tag{2.9}$$

where $X, Y, Z, \Theta, x, y, z, \theta$ are the modified Delaunay variables.

The new Hamiltonian $\widehat{H'}$, resulting from the canonical transformation defined by (2.9), is given by

$$\widehat{H'} = \frac{\mu^2}{2X^2} - \omega_e \Theta + \sum_{l=2}^{\infty} \sum_{m=0}^{l} R'_{lm}, \tag{2.10}$$

where the disturbing potential R'_{lm} is given by

$$R'_{lm} = \sum_{p=0}^{l} \sum_{q=-\infty}^{+\infty} B'_{lmpq}(X, Y, Z) \cos\left(\phi_{lmpq}(x, y, z, \theta)\right). \tag{2.11}$$

Now, consider the commensurability between the Earth rotation angular velocity ω_e and the mean motion $n = \mu^2/X^3$. This commensurability can be expressed as

$$qn - m\omega_e \cong 0, \tag{2.12}$$

considering q and m as integers. The ratio q/m defining the commensurability will be denoted by α. When the commensurability occurs, small divisors arise in the integration of the equations of motion [9]. These periodic terms in the Hamiltonian $\widehat{H'}$ with frequencies $qn - m\omega_e$ are called resonant terms. The other periodic terms are called short- and long-period terms.

The short- and long-period terms can be eliminated from the Hamiltonian $\widehat{H'}$ by applying an averaging procedure [12, 18]:

$$\left\langle \widehat{H'} \right\rangle = \frac{1}{4\pi^2} \int_0^{2\pi} \int_0^{2\pi} \widehat{H'} d\xi_{\text{sp}} d\xi_{\text{lp}}. \tag{2.13}$$

The variables ξ_{sp} and ξ_{lp} represent the short- and long-period terms, respectively, to be eliminated of the Hamiltonian $\widehat{H'}$.

The long-period terms have a combination in the argument ϕ_{lmpq} which involves only the argument of the pericentre ω and the longitude of the ascending node Ω. From (2.10) and (2.11), these terms are represented by the new variables in the following equation:

$$\widehat{H'_{\text{lp}}} = \sum_{l=2}^{\infty} \sum_{m=0}^{l} \sum_{p=0}^{l} \sum_{q=-\infty}^{+\infty} B'_{lmpq}(X, Y, Z) \cos\left((l - 2p)(y - z) + mz\right). \tag{2.14}$$

The short-period terms are identified by the presence of the sidereal time θ and mean anomaly M in the argument ϕ_{lmpq}; in this way, from (2.10) and (2.11), the term $\widehat{H'_{\text{sp}}}$ in the new variables is given by the following equations:

$$\widehat{H'_{\text{sp}}} = \sum_{l=2}^{\infty} \sum_{m=0}^{l} \sum_{p=0}^{l} \sum_{q=-\infty}^{+\infty} B'_{lmpq}(X, Y, Z) \cos\left(q(x - y) - m\theta + \zeta_p\right). \tag{2.15}$$

The term ζ_p represents the other variables in the argument ϕ_{lmpq}, including the argument of the pericentre ω and the longitude of the ascending node Ω, or, in terms of the new variables, $y - z$ and z, respectively.

A reduced Hamiltonian $\widehat{H_r}$ is obtained from the Hamiltonian $\widehat{H'}$ when only secular and resonant terms are considered. The reduced Hamiltonian $\widehat{H_r}$ is given by

$$\begin{aligned}\widehat{H_r} = \frac{\mu^2}{2X^2} - \omega_e\Theta + \sum_{j=1}^{\infty} B'_{2j,0,j,0}(X,Y,Z) \\ + \sum_{l=2}^{\infty}\sum_{m=2}^{l}\sum_{p=0}^{l} B'_{lmp(\alpha m)}(X,Y,Z)\cos\left(\phi_{lmp(\alpha m)}(x,y,z,\theta)\right).\end{aligned} \tag{2.16}$$

Several authors, [11, 15, 19–22], also use this simplified Hamiltonian to study the resonance.

The dynamical system generated from the reduced Hamiltonian, (2.16), is given by

$$\frac{d(X,Y,Z,\Theta)}{dt} = \frac{\partial\widehat{H_r}}{\partial(x,y,z,\theta)}, \qquad \frac{d(x,y,z,\theta)}{dt} = -\frac{\partial\widehat{H_r}}{\partial(X,Y,Z,\Theta)}. \tag{2.17}$$

The equations of motion dX/dt, dY/dt, and dZ/dt defined by (2.17) are

$$\frac{dX}{dt} = -\alpha\sum_{l=2}^{\infty}\sum_{m=2}^{l}\sum_{p=0}^{l} mB'_{lmp(\alpha m)}(X,Y,Z)\sin\left(\phi_{lmp(\alpha m)}(x,y,z,\theta)\right), \tag{2.18}$$

$$\frac{dY}{dt} = -\sum_{l=2}^{\infty}\sum_{m=2}^{l}\sum_{p=0}^{l}(l-2p-m\alpha)B'_{lmp(\alpha m)}(X,Y,Z)\sin\left(\phi_{lmp(\alpha m)}(x,y,z,\theta)\right), \tag{2.19}$$

$$\frac{dZ}{dt} = \sum_{l=2}^{\infty}\sum_{m=2}^{l}\sum_{p=0}^{l}(l-2p-m)B'_{lmp(\alpha m)}(X,Y,Z)\sin\left(\phi_{lmp(\alpha m)}(x,y,z,\theta)\right). \tag{2.20}$$

From (2.18) to (2.20), one can determine the first integral of the system determined by the Hamiltonian $\widehat{H_r}$.

Equation (2.18) can be rewritten as

$$\frac{1}{\alpha}\frac{dX}{dt} = -\sum_{l=2}^{\infty}\sum_{m=2}^{l}\sum_{p=0}^{l} mB'_{lmp(\alpha m)}(X,Y,Z)\sin\left(\phi_{lmp(\alpha m)}(x,y,z,\theta)\right). \tag{2.21}$$

Adding (2.19) and (2.20),

$$\frac{dY}{dt} + \frac{dZ}{dt} = (\alpha-1)\sum_{l=2}^{\infty}\sum_{m=2}^{l}\sum_{p=0}^{l} mB'_{lmp(\alpha m)}(X,Y,Z)\sin\left(\phi_{lmp(\alpha m)}(x,y,z,\theta)\right), \tag{2.22}$$

and substituting (2.21) and (2.22), one obtains

$$\frac{dY}{dt} + \frac{dZ}{dt} = -(\alpha - 1)\frac{1}{\alpha}\frac{dX}{dt}. \tag{2.23}$$

Now, (2.23) is rewritten as

$$\left(1 - \frac{1}{\alpha}\right)\frac{dX}{dt} + \frac{dY}{dt} + \frac{dZ}{dt} = 0. \tag{2.24}$$

In this way, the canonical system of differential equations governed by $\widehat{H_r}$ has the first integral generated from (2.24):

$$\left(1 - \frac{1}{\alpha}\right)X + Y + Z = C_1, \tag{2.25}$$

where C_1 is an integration constant.

Using this first integral, a Mathieu transformation

$$(X, Y, Z, \Theta, x, y, z, \theta) \longrightarrow (X_1, Y_1, Z_1, \Theta_1, x_1, y_1, z_1, \theta_1) \tag{2.26}$$

can be defined.

This transformation is given by the following equations:

$$\begin{aligned} &X_1 = X, \qquad Y_1 = Y, \qquad Z_1 = \left(1 - \frac{1}{\alpha}\right)X + Y + Z, \quad \Theta_1 = \Theta, \\ &x_1 = x - \left(1 - \frac{1}{\alpha}\right)z, \qquad y_1 = y - z, \qquad z_1 = z, \qquad \theta_1 = \theta. \end{aligned} \tag{2.27}$$

The subscript 1 denotes the new set of canonical variables. Note that $Z_1 = C_1$, and the z_1 is an ignorable variable. So the order of the dynamical system is reduced in one degree of freedom.

Substituting the new set of canonical variables, X_1, Y_1, Z_1, Θ_1, x_1, y_1, z_1, θ_1, in the reduced Hamiltonian given by (2.16), one gets the resonant Hamiltonian. The word "resonant" is used to denote the Hamiltonian H_{rs} which is valid for any resonance. The periodic terms in this Hamiltonian are resonant terms. The Hamiltonian H_{rs} is given by

$$\begin{aligned} H_{\mathrm{rs}} = {} & \frac{\mu^2}{2X_1^2} - \omega_e\Theta_1 + \sum_{j=1}^{\infty} B_{2j,0,j,0}(X_1, Y_1, C_1) \\ & + \sum_{l=2}^{\infty}\sum_{m=2}^{l}\sum_{p=0}^{l} B_{lmp,(\alpha m)}(X_1, Y_1, C_1)\cos\left(\phi_{lmp(\alpha m)}(x_1, y_1, \theta_1)\right). \end{aligned} \tag{2.28}$$

The Hamiltonian H_{rs} has all resonant frequencies, relative to the commensurability α, where the $\phi_{lmp(\alpha m)}$ argument is given by

$$\phi_{lmp(\alpha m)} = m(\alpha x_1 - \theta_1) + (l - 2p - \alpha m)y_1 - \phi_{lmp(\alpha m)0}, \tag{2.29}$$

with

$$\phi_{lmp(\alpha m)0} = m\lambda_{lm} - (l - m)\frac{\pi}{2}. \tag{2.30}$$

The secular and resonant terms are given, respectively, by $B_{2j,0,j,0}(X_1, Y_1, C_1)$ and $B_{lmp(\alpha m)}(X_1, Y_1, C_1)$.

Each one of the frequencies contained in dx_1/dt, dy_1/dt, $d\theta_1/dt$ is related, through the coefficients l, m, to a tesseral harmonic J_{lm}. By varying the coefficients l, m, p and keeping q/m fixed, one finds all frequencies $d\phi_{1,lmp(\alpha m)}/dt$ concerning a specific resonance.

From H_{rs}, taking, $j = 1, 2$, $l = 2, 4$, $m = 2$, $\alpha = 1/2$, and $p = 0, 1, 2, 3$, one gets

$$\begin{aligned}
\widehat{H_1} = {} & \frac{\mu^2}{2X_1^2} - \omega_e\Theta_1 + B_{1,2010}(X_1, Y_1, C_1) + B_{1,4020}(X_1, Y_1, C_1) \\
& + B_{1,2201}(X_1, Y_1, C_1)\cos(x_1 - 2\theta_1 + y_1 - 2\lambda_{22}) \\
& + B_{1,2211}(X_1, Y_1, C_1)\cos(x_1 - 2\theta_1 - y_1 - 2\lambda_{22}) \\
& + B_{1,2221}(X_1, Y_1, C_1)\cos(x_1 - 2\theta_1 - 3y_1 - 2\lambda_{22}) \\
& + B_{1,4211}(X_1, Y_1, C_1)\cos(x_1 - 2\theta_1 + y_1 - 2\lambda_{42} + \pi) \\
& + B_{1,4221}(X_1, Y_1, C_1)\cos(x_1 - 2\theta_1 - y_1 - 2\lambda_{42} + \pi) \\
& + B_{1,4231}(X_1, Y_1, C_1)\cos(x_1 - 2\theta_1 - 3y_1 - 2\lambda_{42} + \pi).
\end{aligned} \tag{2.31}$$

The Hamiltonian $\widehat{H_1}$ is defined considering a fixed resonance and three different critical angles associated to the tesseral harmonic J_{22}; the critical angles associated to the tesseral harmonic J_{42} have the same frequency of the critical angles associated to the J_{22} with a difference in the phase. The other terms in H_{rs} are considered as short-period terms.

Table 1 shows the resonant coefficients used in the Hamiltonian $\widehat{H_1}$.

Finally, a last transformation of variables is done, with the purpose of writing the resonant angle explicitly. This transformation is defined by

$$\begin{aligned}
&X_4 = X_1, \qquad Y_4 = Y_1, \qquad \Theta_4 = \Theta_1 + 2X_1, \\
&x_4 = x_1 - 2\theta_1, \qquad y_4 = y_1, \qquad \theta_4 = \theta_1.
\end{aligned} \tag{2.32}$$

Table 1: Resonant coefficients.

Degree (l)	Order (m)	p	q
2	2	0	1
2	2	1	1
2	2	2	1
4	2	1	1
4	2	2	1
4	2	3	1

So, considering (2.31) and (2.32), the Hamiltonian H_4 is found to be

$$\begin{aligned} H_4 = {} & \frac{\mu^2}{2X_4^2} - \omega_e(\Theta_4 - 2X_4) + B_{4,2010}(X_4, Y_4, C_1) + B_{4,4020}(X_4, Y_4, C_1) \\ & + B_{4,2201}(X_4, Y_4, C_1)\cos(x_4 + y_4 - 2\lambda_{22}) \\ & + B_{4,2211}(X_4, Y_4, C_1)\cos(x_4 - y_4 - 2\lambda_{22}) \\ & + B_{4,2221}(X_4, Y_4, C_1)\cos(x_4 - 3y_4 - 2\lambda_{22}) \\ & + B_{4,4211}(X_4, Y_4, C_1)\cos(x_4 + y_4 - 2\lambda_{42} + \pi) \\ & + B_{4,4221}(X_4, Y_4, C_1)\cos(x_4 - y_4 - 2\lambda_{42} + \pi) \\ & + B_{4,4231}(X_4, Y_4, C_1)\cos(x_4 - 3y_4 - 2\lambda_{42} + \pi), \end{aligned} \tag{2.33}$$

with $\omega_e\Theta_4$ constant and

$$B_{4,2010} = \frac{\mu^4}{X_4^6} {a_e}^2 J_{20}\left(-\frac{3}{4}\,\frac{(C_1 + 2X_4)^2}{(X_4 + Y_4)^2} + \frac{1}{4}\right)\left(1 + \frac{3}{2}\,\frac{-{Y_4}^2 - 2X_4Y_4}{{X_4}^2}\right), \tag{2.34}$$

$$\begin{aligned} B_{4,4020} = {} & \frac{\mu^6}{X_4^{10}} {a_e}^4 J_{40}\left(\frac{105}{64}\left(1 - \frac{(C_1 + 2X_4)^2}{(X_4 + Y_4)^2}\right)^2 - \frac{3}{2} + \frac{15}{8}\,\frac{(C_1 + 2X_4)^2}{(X_4 + Y_4)^2}\right) \\ & \times\left(1 + 5\,\frac{-{Y_4}^2 - 2X_4Y_4}{{X_4}^2}\right), \end{aligned} \tag{2.35}$$

$$B_{4,2201} = \frac{21}{8X_4^7}\,\mu^4 {a_e}^2 J_{22}\left(1 + \frac{C_1 + 2X_4}{X_4 + Y_4}\right)^2\sqrt{-{Y_4}^2 - 2X_4Y_4}, \tag{2.36}$$

$$B_{4,2211} = \frac{3}{2X_4^7}\,\mu^4 {a_e}^2 J_{22}\left(\frac{3}{2} - \frac{3}{2}\,\frac{(C_1 + 2X_4)^2}{(X_4 + Y_4)^2}\right)\sqrt{-{Y_4}^2 - 2X_4Y_4}, \tag{2.37}$$

$$B_{4,2221} = -\frac{3}{8X_4^7}\,\mu^4 {a_e}^2 J_{22}\left(1-\frac{C_1+2X_4}{X_4+Y_4}\right)^2\sqrt{-{Y_4}^2-2X_4Y_4}, \tag{2.38}$$

$$\begin{aligned} B_{4,4211} = \frac{9}{2X_4^{11}}\,\mu^6 {a_e}^4 J_{42}\Bigg(&\frac{35}{27}\left(1-\frac{(C_1+2X_4)^2}{(X_4+Y_4)^2}\right)(C_1+2X_4)\\ &\times\left(1+\frac{C_1+2X_4}{X_4+Y_4}\right)(X_4+Y_4)^{-1}\\ &-\frac{15}{8}\left(1+\frac{C_1+2X_4}{X_4+Y_4}\right)^2\Bigg)\sqrt{-{Y_4}^2-2X_4Y_4}, \end{aligned} \tag{2.39}$$

$$\begin{aligned} B_{4,4221} = \frac{5}{2X_4^{11}}\mu^6 {a_e}^4 J_{42}\Bigg(&\frac{105}{16}\left(1-\frac{(C_1+2X_4)^2}{(X_4+Y_4)^2}\right)\left(1-3\,\frac{(C_1+2X_4)^2}{(X_4+Y_4)^2}\right)\\ &+\frac{15}{4}-\frac{15}{4}\frac{(C_1+2X_4)^2}{(X_4+Y_4)^2}\Bigg)\sqrt{-{Y_4}^2-2X_4Y_4}, \end{aligned} \tag{2.40}$$

$$\begin{aligned} B_{4,4231} = \frac{\mu^6}{X_4^{10}}{a_e}^4 J_{42}\Bigg(&-\frac{35}{27}\left(1-\frac{(C_1+2X_4)^2}{(X_4+Y_4)^2}\right)(C_1+2X_4)\\ &\times\left(1-\frac{C_1+2X_4}{X_4+Y_4}\right)(X_4+Y_4)^{-1}-\frac{15}{8}\left(1-\frac{C_1+2X_4}{X_4+Y_4}\right)^2\Bigg)\\ &\times\left(\frac{1}{2}\,\frac{\sqrt{-{Y_4}^2-2X_4Y_4}}{X_4}+\frac{33}{16}\,\frac{-{Y_4}^2-2X_4Y_4}{{X_4}^2}\right). \end{aligned} \tag{2.41}$$

Since the term $\omega_e\Theta_4$ is constant, it plays no role in the equations of motion, and a new Hamiltonian can be introduced,

$$\widehat{H_4} = H_4 + \omega_e\Theta_4. \tag{2.42}$$

The dynamical system described by $\widehat{H_4}$ is given by

$$\frac{d(X_4,Y_4)}{dt} = \frac{\partial\widehat{H_4}}{\partial(x_4,y_4)}, \quad \frac{d(x_4,y_4)}{dt} = -\frac{\partial\widehat{H_4}}{\partial(X_4,Y_4)}. \tag{2.43}$$

Table 2: The zonal and tesseral harmonics.

Zonal harmonics	Tesseral harmonics
$J_{20} = 1.0826 \times 10^{-3}$	$J_{22} = 1.8154 \times 10^{-6}$
$J_{40} = -1.6204 \times 10^{-6}$	$J_{42} = 1.6765 \times 10^{-7}$

The zonal harmonics used in (2.34) and (2.35) and the tesseral harmonics used in (2.36) to (2.41) are shown in Table 2.

The constant of integration C_1 in (2.34) to (2.41) is given, in terms of the initial values of the orbital elements, a_o, e_o, and I_o, by

$$C_1 = \sqrt{\mu a_o}\left(\sqrt{1-e_o^2}\cos(I_o) - 2\right) \tag{2.44}$$

or, in terms of the variables X_4 and Y_4,

$$C_1 = X_4(\cos(I_o) - 2) + Y_4\cos(I_o). \tag{2.45}$$

In Section 4, some results of the numerical integration of (2.43) are shown.

3. Lyapunov Exponents

The estimation of the chaoticity of orbits is very important in the studies of dynamical systems, and possible irregular motions can be analyzed by Lyapunov exponents [23].

In this work, "Gram-Schmidt's method," described in [23–26], will be applied to compute the Lyapunov exponents. A brief description of this method is presented in what follows.

The dynamical system described by (2.43) can be rewritten as

$$\begin{aligned}
\frac{dX_4}{dt} &= P_1(X_4, Y_4, x_4, y_4; C_1),\\
\frac{dY_4}{dt} &= P_2(X_4, Y_4, x_4, y_4; C_1),\\
\frac{dx_4}{dt} &= P_3(X_4, Y_4, x_4, y_4; C_1),\\
\frac{dy_4}{dt} &= P_4(X_4, Y_4, x_4, y_4; C_1).
\end{aligned} \tag{3.1}$$

Introducing

$$z = \begin{pmatrix} X_4 \\ Y_4 \\ x_4 \\ y_4 \end{pmatrix}, \qquad Z = \begin{pmatrix} P_1 \\ P_2 \\ P_3 \\ P_4 \end{pmatrix}. \tag{3.2}$$

Equations (3.2) can be put in the form

$$\frac{dz}{dt} = Z(z). \tag{3.3}$$

The variational equations, associated to the system of differential equations (3.3), are given by

$$\frac{d\zeta}{dt} = J\zeta, \tag{3.4}$$

where $J = (\partial Z/\partial z)$ is the Jacobian.

The total number of differential equations used in this method is $n(n+1)$, n represents the number of the motion equations describing the problem, in this case four. In this way, there are twenty differential equations, four are motion equations of the problem and sixteen are variational equations described by (3.4).

The dynamical system represented by (3.3) and (3.4) is numerically integrated and the neighboring trajectories are studied using the Gram-Schmidt orthonormalization to calculate the Lyapunov exponents.

The method of the Gram-Schmidt orthonormalization can be seen in [25, 26] with more details. A simplified denomination of the method is described as follows.

Considering the solutions to (3.4) as $\mathbf{u}_\kappa(t)$, the integration in the time τ begins from initial conditions $\mathbf{u}_\kappa(t_0) = \mathbf{e}_\kappa(t_0)$, an orthonormal basis.

At the end of the time interval, the volumes of the κ-dimensional ($\kappa = 1, 2, \ldots, N$) produced by the vectors $\mathbf{u}_\kappa$ are calculated by

$$V_\kappa = \left\| \bigwedge_{j=1}^{\kappa} \mathbf{u}_j(t) \right\|, \tag{3.5}$$

where $\bigwedge$ is the outer product and $\|\cdot\|$ is a norm.

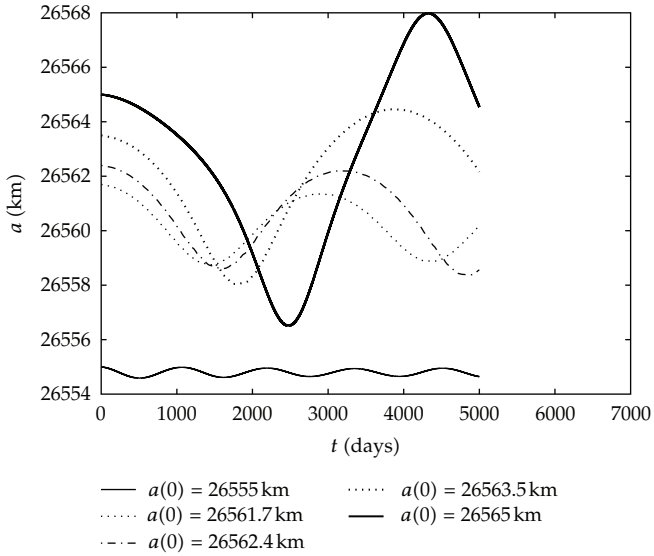

Figure 1: Time behavior of the semimajor axis for different values of C_1 given in Table 3.

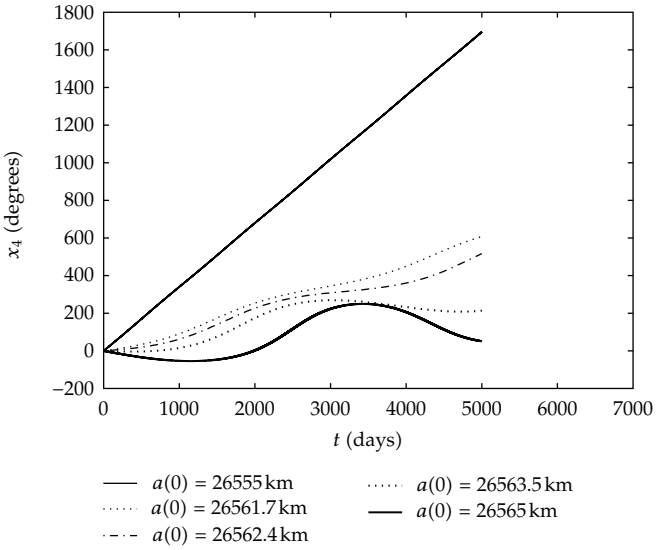

Figure 2: Time behavior of x_4 angle for different values of C_1 given in Table 3.

In this way, the vectors $\mathbf{u}_\kappa$ are orthonormalized by Gram-Schmidt method. In other words, new orthonormal vectors $\mathbf{e}_\kappa(t_0 + \tau)$ are calculated, in general, according to

$$\mathbf{e}_\kappa = \frac{\mathbf{u}_\kappa - \sum_{j=1}^{\kappa-1} (\mathbf{u}_\kappa \cdot \mathbf{e}_j)\mathbf{e}_j}{\left\| \mathbf{u}_\kappa - \sum_{j=1}^{\kappa-1} (\mathbf{u}_\kappa \cdot \mathbf{e}_j)\mathbf{e}_j \right\|}. \tag{3.6}$$

Table 3: Values of the constant of integration C_1 for $e = 0.001$, $I = 55°$ and different values for semimajor axis.

$a(0) \times 10^3$(m)	$C_1 \times 10^{11}$(m^2/s)
26555.000	−1.467543158
26561.700	−1.467728282
26562.400	−1.467747623
26563.500	−1.467778013
26565.000	−1.467819454

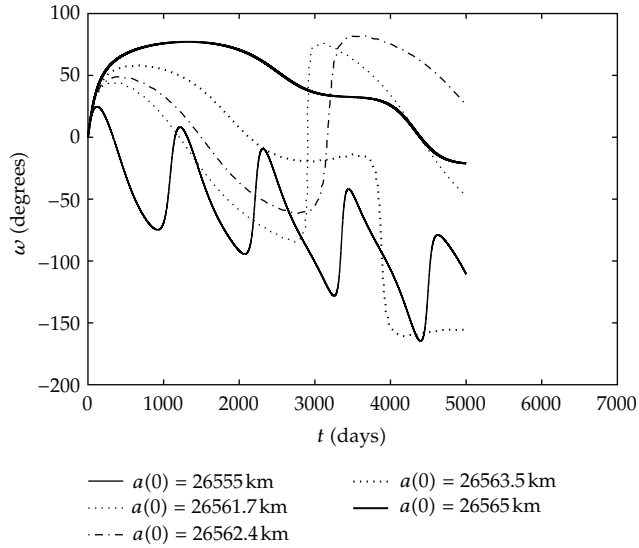

Figure 3: Time behavior of the argument of pericentre for different values of C_1 given in Table 3.

The Gram-Schmidt method makes invariant the κ-dimensional subspace produced by the vectors $\mathbf{u}_1, \mathbf{u}_2, \mathbf{u}_3, \ldots, \mathbf{u}_\kappa$ in constructing the new κ-dimensional subspace spanned by the vectors $\mathbf{e}_1, \mathbf{e}_2, \mathbf{e}_3, \ldots, \mathbf{e}_\kappa$.

With new vector $\mathbf{u}_\kappa(t_0 + \tau) = \mathbf{e}_\kappa(t_0 + \tau)$, the integration is reinitialized and carried forward to $t = t_0 + 2\tau$. The whole cycle is repeated over a long-time interval. The theorems guarantee that the κ-dimensional Lyapunov exponents are calculated by [25, 26]:

$$\lambda(\kappa) = \lim_{n\to\infty} \frac{1}{n\tau} \sum_{j=1}^{n} \frac{\ln\left(V_\kappa(t_0 + j\tau)\right)}{\ln\left(V_\kappa(t_0 + (j-1)\tau)\right)}. \tag{3.7}$$

The theory states that if the Lyapunov exponent tends to a positive value, the orbit is chaotic.

In the next section are shown some results about the Lyapunov exponents.

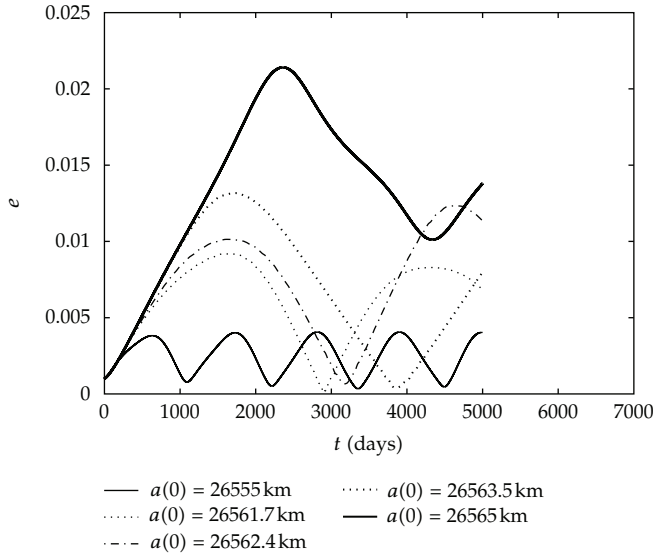

Figure 4: Time behavior of the eccentricity for different values of C_1 given in Table 3.

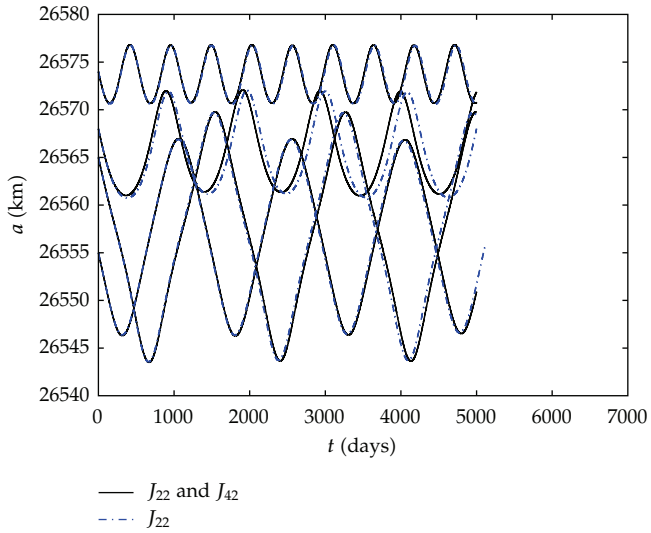

Figure 5: Time behavior of the semimajor axis for different values of C_1 given in Table 4.

4. Results

Figures 1, 2, 3, and 4 show the time behavior of the semimajor axis, x_4 angle, argument of perigee and of the eccentricity, according to the numerical integration of the motion equations, (2.43), considering three different resonant angles together: ϕ_{2201}, ϕ_{2211}, and ϕ_{2221} associated to J_{22}, and three angles, ϕ_{4211}, ϕ_{4221}, and ϕ_{4231} associated to J_{42}, with the same frequency of the resonant angles related to the J_{22}, but with different phase. The initial conditions corresponding to variables X_4 and Y_4 are defined for $e_o = 0.001$, $I_o = 55°$, and a_o given in Table 3.

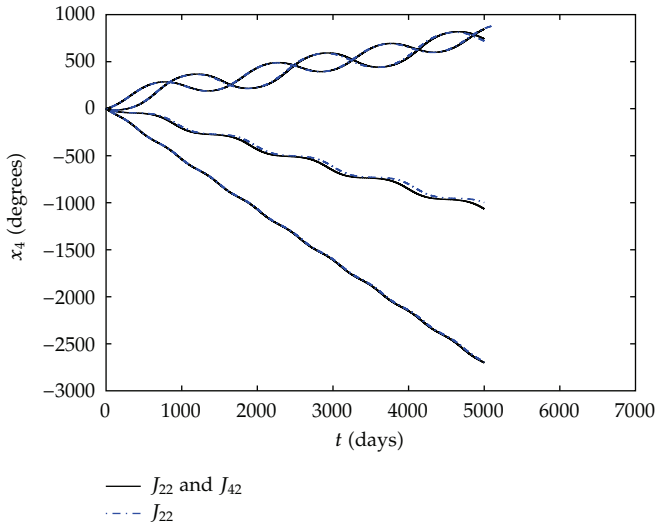

Figure 6: Time behavior of x_4 angle for different values of C_1 given in Table 4.

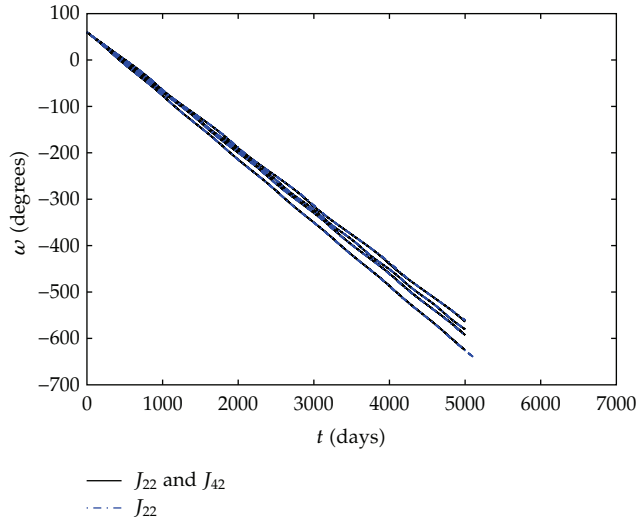

Figure 7: Time behavior of the argument of pericentre for different values of C_1 given in Table 4.

Table 4: Values of the constant of integration C_1 for $e = 0.05$, $I = 10°$, and different values for semimajor axis.

$a(0) \times 10^3$(m)	$C_1 \times 10^{11}$ (m^2/s)
26555.000	−1.045724331
26565.000	−1.045921210
26568.000	−1.045980267
26574.000	−1.046098370

The initial conditions of the variables x_4 and y_4 are 0° and 0°, respectively. Table 3 shows the values of C_1 corresponding to the given initial conditions.

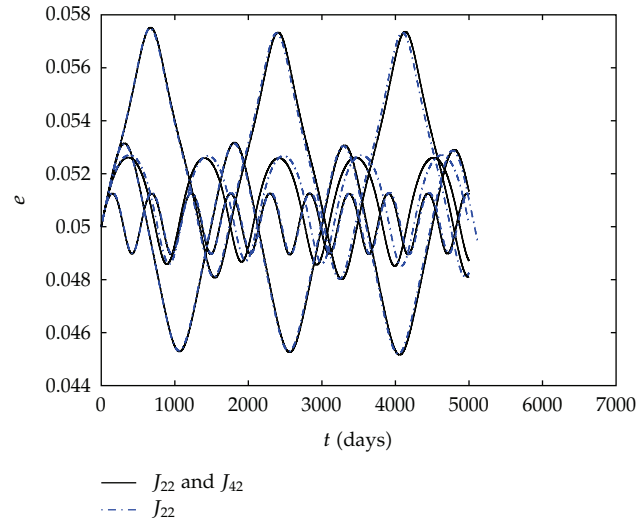

Figure 8: Time behavior of the eccentricity for different values of C_1 given in Table 4.

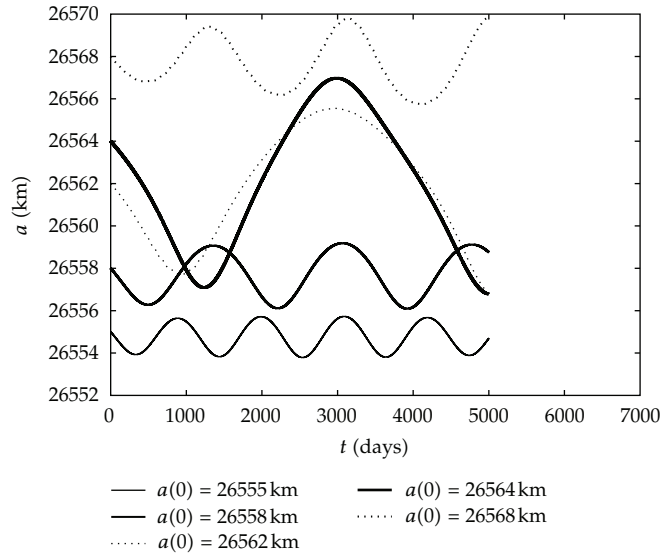

Figure 9: Time behavior of the semimajor axis for different values of C_1 given in Table 5.

Figures 5, 6, 7, and 8 show the time behavior of the semimajor axis, x_4 angle, argument of perigee and of the eccentricity for two different cases. The first case considers the critical angles ϕ_{2201}, ϕ_{2211}, and ϕ_{2221}, associated to the tesseral harmonic J_{22}, and the second case considers the critical angles associated to the tesseral harmonics J_{22} and J_{42}. The angles associated to the J_{42}, ϕ_{4211}, ϕ_{4221}, and ϕ_{4231}, have the same frequency of the critical angles associated to the J_{22} with a different phase. The initial conditions corresponding to variables X_4 and Y_4 are defined for $e_o = 0.05$, $I_o = 10°$, and a_o given in Table 4. The initial conditions of the variables x_4 and y_4 are 0° and 60°, respectively. Table 4 shows the values of C_1 corresponding to the given initial conditions.

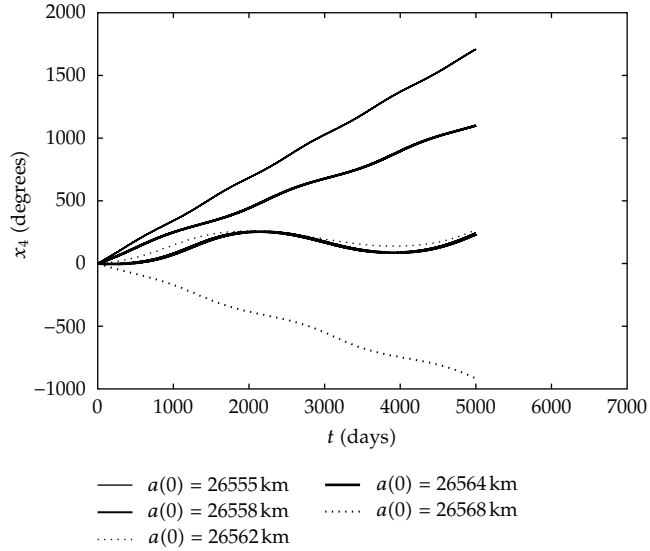

Figure 10: Time behavior of x_4 angle for different values of C_1 given in Table 5.

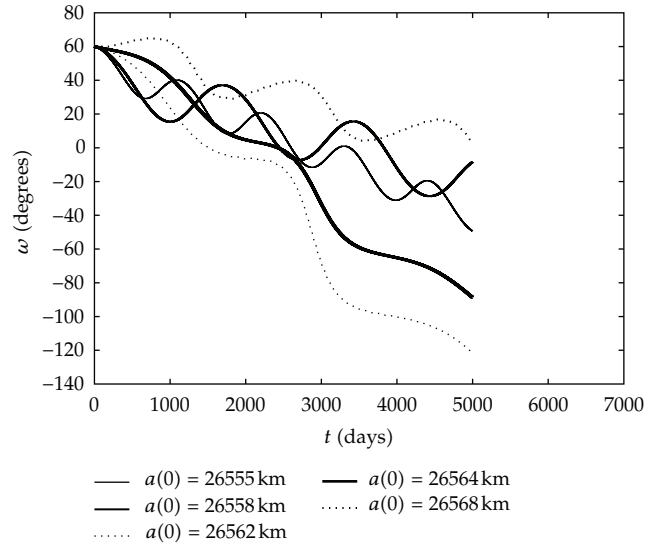

Figure 11: Time behavior of the argument of pericentre for different values of C_1 given in Table 5.

Analyzing Figures 5–8, one can observe a correction in the orbits when the terms related to the tesseral harmonic J_{42} are added to the model. Observing, by the percentage, the contribution of the amplitudes of the terms $B_{4,4211}$, $B_{4,4221}$, and $B_{4,4231}$, in each critical angle studied, is about 1,66% up to 4,94%. In fact, in the studies of the perturbations in the artificial satellites motion, the accuracy is important, since adding different tesseral and zonal harmonics to the model, one can have a better description about the orbital motion.

Figures 9, 10, 11, and 12 show the time behavior of the semimajor axis, x_4 angle, argument of perigee and of the eccentricity, according to the numerical integration of the motion equations, (2.43), considering three different resonant angles together; ϕ_{2201}, ϕ_{2211}, and ϕ_{2221}

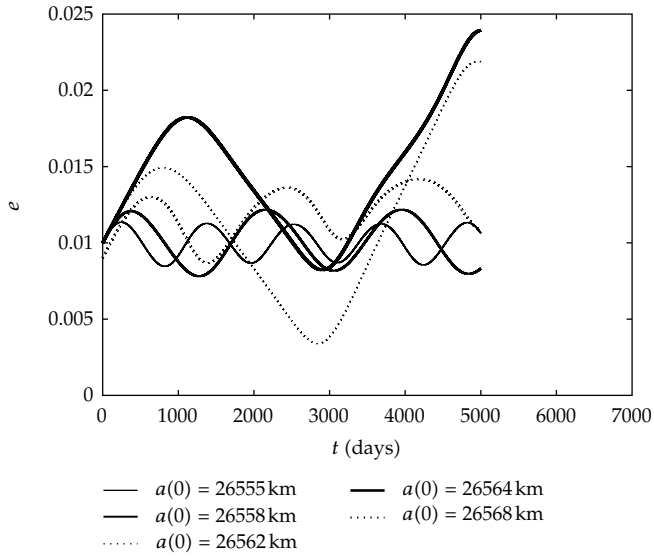

Figure 12: Time behavior of the eccentricity for different values of C_1 given in Table 5.

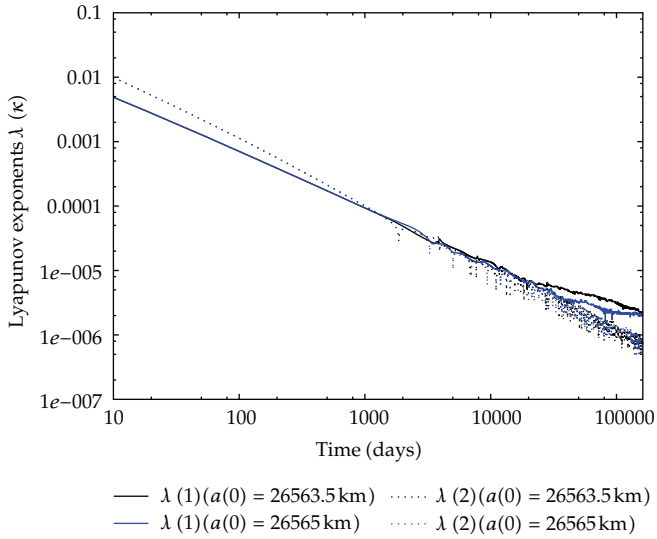

Figure 13: Lyapunov exponents $\lambda(1)$ and $\lambda(2)$, corresponding to the variables X_4 and Y_4, respectively, for $C_1 = -1.467778013 \times 10^{11}\,\mathrm{m}^2/\mathrm{s}$ and $C_1 = -1.467819454 \times 10^{11}\,\mathrm{m}^2/\mathrm{s}$, $x_4 = 0°$ and $y_4 = 0°$.

associated to J_{22} and three angles ϕ_{4211}, ϕ_{4221}, and ϕ_{4231} associated to J_{42}. The initial conditions corresponding to variables X_4 and Y_4 are defined for $e_o = 0.01$, $I_o = 55°$, and a_o given in Table 5. The initial conditions of the variables x_4 and y_4 are 0° and 60°, respectively. Table 5 shows the values of C_1 corresponding to the given initial conditions.

Analyzing Figures 1–12, one can observe possible irregular motions in Figures 1–4, specifically considering values for $C_1 = -1.467778013 \times 10^{11}\,\mathrm{m}^2/\mathrm{s}$ and $C_1 = -1.467819454 \times 10^{11}\,\mathrm{m}^2/\mathrm{s}$, and, in Figures 9–12, for $C_1 = -1.467765786 \times 10^{11}\,\mathrm{m}^2/\mathrm{s}$ and $C_1 = -1.467821043 \times 10^{11}\,\mathrm{m}^2/\mathrm{s}$. These curves will be analyzed by the Lyapunov exponents in a specified time verifying the possible regular or chaotic motions.

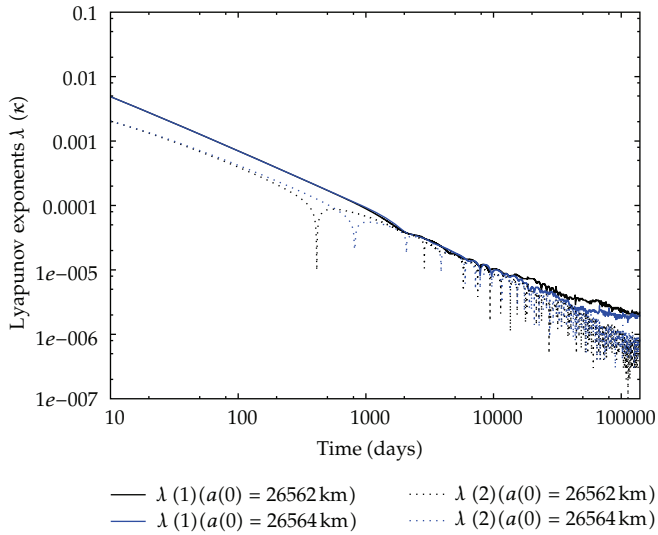

Figure 14: Lyapunov exponents $\lambda(1)$ and $\lambda(2)$, corresponding to the variables X_4 and Y_4, respectively, for $C_1 = -1.467765786 \times 10^{11}\,\mathrm{m}^2/\mathrm{s}$ and $C_1 = -1.467821043 \times 10^{11}\,\mathrm{m}^2/\mathrm{s}$, $x_4 = 0°$ and $y_4 = 60°$.

Table 5: Values of the constant of integration C_1 for $e = 0.01$, $I = 55°$, and different values for semimajor axis.

$a(0) \times 10^3(\mathrm{m})$	$C_1 \times 10^{11}(\mathrm{m}^2/\mathrm{s})$
26555.000	−1.467572370
26558.000	−1.467655265
26562.000	−1.467765786
26564.000	−1.467821043
26568.000	−1.467931552

Figures 13 and 14 show the time behavior of the Lyapunov exponents for two different cases, according to the initial values of Figures 1–4 and 9–12. The dynamical system involves the zonal harmonics J_{20} and J_{40} and the tesseral harmonics J_{22} and J_{42}. The method used in this work for the study of the Lyapunov exponents is described in Section 3. In Figure 13, the initial values for C_1, x_4, and y_4 are $C_1 = -1.467778013 \times 10^{11}\,\mathrm{m}^2/\mathrm{s}$ and $C_1 = -1.467819454 \times 10^{11}\,\mathrm{m}^2/\mathrm{s}$, $x_4 = 0°$ and $y_4 = 0°$, respectively. In Figure 14, the initial values for C_1, x_4, and y_4 are $C_1 = -1.467765786 \times 10^{11}\,\mathrm{m}^2/\mathrm{s}$ and $C_1 = -1.467821043 \times 10^{11}\,\mathrm{m}^2/\mathrm{s}$, $x_4 = 0°$ and $y_4 = 60°$, respectively. In each case are used two different values for semimajor axis corresponding to neighboring orbits shown previously in Figures 1–4 and 9–12.

Figures 13 and 14 show Lyapunov exponents for neighboring orbits. The time used in the calculations of the Lyapunov exponents is about 150.000 days. For this time, it can be observed in Figure 13 that $\lambda(1)$, corresponding to the initial value $a(0) = 26565.0\,\mathrm{km}$, tends to a positive value, evidencing a chaotic region. On the other hand, analyzing the same Figure 13, $\lambda(1)$, corresponding to the initial value $a(0) = 26563.5\,\mathrm{km}$, does not show a stabilization around the some positive value, in this specified time. Probably, the time is not sufficient for a stabilization in some positive value, or $\lambda(1)$, initial value $a(0) = 26563.5\,\mathrm{km}$, tends to a negative value, evidencing a regular orbit. Analyzing now Figure 14, it can be verified that $\lambda(1)$, corresponding to the initial value $a(0) = 26564.0\,\mathrm{km}$, tends to a positive value, it contrasts

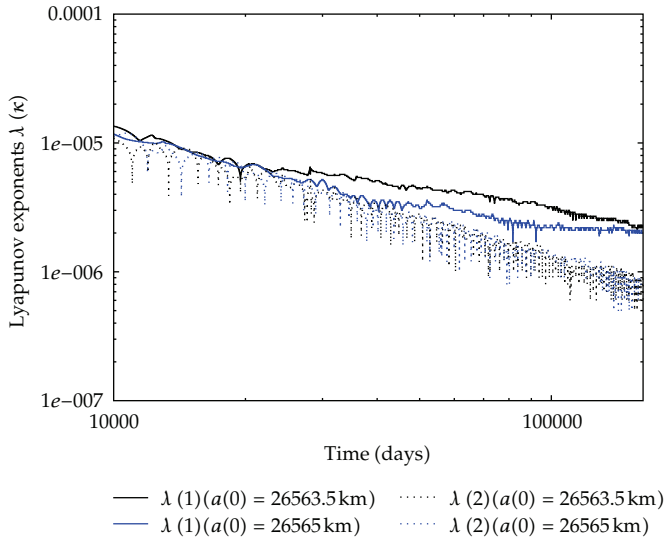

Figure 15: Lyapunov exponents $\lambda(1)$ and $\lambda(2)$, corresponding to the variables X_4 and Y_4, respectively, for $C_1 = -1.467778013 \times 10^{11}\,\mathrm{m}^2/\mathrm{s}$ and $C_1 = -1.467819454 \times 10^{11}\,\mathrm{m}^2/\mathrm{s}$, $x_4 = 0°$ and $y_4 = 0°$.

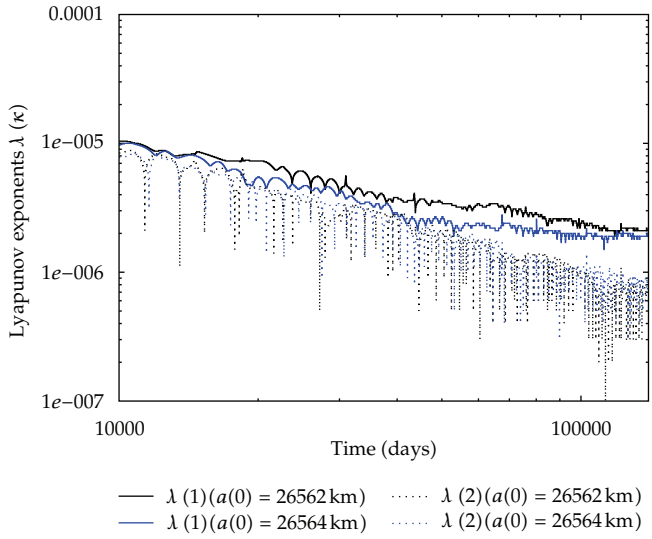

Figure 16: Lyapunov exponents $\lambda(1)$ and $\lambda(2)$, corresponding to the variables X_4 and Y_4, respectively, for $C_1 = -1.467765786 \times 10^{11}\,\mathrm{m}^2/\mathrm{s}$ and $C_1 = -1.467821043 \times 10^{11}\,\mathrm{m}^2/\mathrm{s}$, $x_4 = 0°$ and $y_4 = 60°$.

with $\lambda(1)$, initial value $a(0) = 26562.0$ km. Comparing Figure 13 with Figure 14, it is observed that the Lyapunov exponents in Figure 14 has an amplitude of oscillation greater than the Lyapunov exponents in Figure 13. Analyzing this fact, it is probable that the necessary time for the Lyapunov exponent $\lambda(2)$, in Figure 14, to stabilize in some positive value is greater than the necessary time for the $\lambda(2)$ in Figure 13.

Rescheduling the axes of Figures 13 and 14, as described in Figures 15 and 16, respectively, the Lyapunov exponents tending to a positive value can be better visualized.

5. Conclusions

In this work, the dynamical behavior of three critical angles associated to the 2 : 1 resonance problem in the artificial satellites motion has been investigated.

The results show the time behavior of the semimajor axis, argument of perigee and eccentricity. In the numerical integration, different cases are studied, using three critical angles together: ϕ_{2201}, ϕ_{2211}, and ϕ_{2221} associated to J_{22} and ϕ_{4211}, ϕ_{4221}, and ϕ_{4231} associated to the J_{42}.

In the simulations considered in the work, four cases show possible irregular motions for $C_1 = -1.467778013 \times 10^{11}\,\mathrm{m}^2/\mathrm{s}$, $C_1 = -1.467819454 \times 10^{11}\,\mathrm{m}^2/\mathrm{s}$, $C_1 = -1.467765786 \times 10^{11}\,\mathrm{m}^2/\mathrm{s}$, and $C_1 = -1.467821043 \times 10^{11}\,\mathrm{m}^2/\mathrm{s}$. Studying the Lyapunov exponents, two cases show chaotic motions for $C_1 = -1.467819454 \times 10^{11}\,\mathrm{m}^2/\mathrm{s}$ and $C_1 = -1.467821043 \times 10^{11}\,\mathrm{m}^2/\mathrm{s}$.

Analyzing the contribution of the terms related to the J_{42}, it is observed that, for the value of $C_1 = -1.045724331 \times 10^{11}\,\mathrm{m}^2/\mathrm{s}$, the amplitudes of the terms $B_{4,4211}$, $B_{4,4221}$, and $B_{4,4231}$ are greater than the other values of C_1. In other words, for bigger values of semimajor axis, it is observed a smaller contribution of the terms related to the tesseral harmonic J_{42}.

The theory used in this paper for the 2 : 1 resonance can be applied for any resonance involving some artificial Earth satellite.

Acknowledgments

This work was accomplished with support of the FAPESP under the Contract no. 2009/00735-5 and 2006/04997-6, SP Brazil, and CNPQ (Contracts 300952/2008-2 and 302949/2009-7).

References

[1] M. B. Morando, "Orbites de resonance des satellites de 24h," *Bulletin of the American Astronomical Society*, vol. 24, pp. 47–67, 1963.

[2] L. Blitzer, "Synchronous and resonant satellite orbits associated with equatorial ellipticity," *Journal of Advanced Robotic Systems*, vol. 32, pp. 1016–1019, 1963.

[3] B. Garfinkel, "The disturbing function for an artificial satellite," *The Astronomical Journal*, vol. 70, no. 9, pp. 688–704, 1965.

[4] B. Garfinkel, "Tesseral harmonic perturbations of an artificial satellite," *The Astronomical Journal*, vol. 70, pp. 784–786, 1965.

[5] B. Garfinkel, "Formal solution in the problem of small divisors," *The Astronomical Journal*, vol. 71, pp. 657–669, 1966.

[6] G. S. Gedeon and O. L. Dial, "Along-track oscillations of a satellite due to tesseral harmonics," *AIAA Journal*, vol. 5, pp. 593–595, 1967.

[7] G. S. Gedeon, B. C. Douglas, and M. T. Palmiter, "Resonance effects on eccentric satellite orbits," *Journal of the Astronautical Sciences*, vol. 14, pp. 147–157, 1967.

[8] G. S. Gedeon, "Tesseral resonance effects on satellite orbits," *Celestial Mechanics*, vol. 1, pp. 167–189, 1969.

[9] M. T. Lane, "An analytical treatment of resonance effects on satellite orbits," *Celestial Mechanics*, vol. 42, pp. 3–38, 1988.

[10] A. Jupp, "A solution of the ideal resonance problem for the case of libration," *The Astronomical Journal*, vol. 74, pp. 35–43, 1969.

[11] T. A. Ely and K. C. Howell, "Long-term evolution of artificial satellite orbits due to resonant tesseral harmonics," *Journal of the Astronautical Sciences*, vol. 44, pp. 167–190, 1996.

[12] D. M. Sanckez, T. Yokoyama, P. I. O. Brasil, and R. R. Cordeiro, "Some initial conditions for disposed satellites of the systems GPS and galileo constellations," *Mathematical Problems in Engineering*, vol. 2009, Article ID 510759, 22 pages, 2009.

[13] L. D. D. Ferreira and R. Vilhena de Moraes, "GPS satellites orbits: resonance," *Mathematical Problems in Engineering*, vol. 2009, Article ID 347835, 12 pages, 2009.
[14] J. C. Sampaio, R. Vilhena de Moraes, and S. S. Fernandes, "Artificial satellites dynamics: resonant effects," in *Proceedings of the 22nd International Symposium on Space Flight Dynamics*, São José dos Campos, Brazil, 2011.
[15] A. G. S. Neto, *Estudo de Órbitas Ressonantes no Movimento de Satélites Artificiais*, Tese de Mestrado, ITA, 2006.
[16] J. P. Osorio, *Perturbações de Órbitas de Satélites no Estudo do Campo Gravitacional Terrestre*, Imprensa Portuguesa, Porto, Portugal, 1973.
[17] W. M. Kaula, *Theory of Satellite Geodesy: Applications of Satellites to Geodesy*, Blaisdel, Waltham, Mass, USA, 1966.
[18] A. E. Roy, *Orbital Motion*, Institute of Physics Publishing Bristol and Philadelphia, 3rd edition, 1988.
[19] P. H. C. N. Lima Jr., *Sistemas Ressonantes a Altas Excentricidades no Movimento de Satélites Artificiais*, Tese de Doutorado, Instituto Tecnológico de Aeronáutica, 1998.
[20] P. R. Grosso, *Movimento Orbital de um Satélite Artificial em Ressonância 2:1*, Tese de Mestrado, Instituto Tecnológico de Aeronáutica, 1989.
[21] J. K. S. Formiga and R. Vilhena de Moraes, "Dynamical systems: an integrable kernel for resonance effects," *Journal of Computational Interdisciplinary Sciences*, vol. 1, no. 2, pp. 89–94, 2009.
[22] R. Vilhena de Moraes, K. T. Fitzgibbon, and M. Konemba, "Influence of the 2:1 resonance in the orbits of GPS satellites," *Advances in Space Research*, vol. 16, no. 12, pp. 37–40, 1995.
[23] F. Christiansen and H. H. Rugh, "Computing lyapunov spectra with continuous gram-schmidt orthonormalization," *Nonlinearity*, vol. 10, no. 5, pp. 1063–1072, 1997.
[24] L. Qun-Hong and T. Jie-Yan, "Lyapunov exponent calculation of a two-degree-of-freedom vibro-impact system with symmetrical rigid stops," *Chinese Physics B*, vol. 20, no. 4, Article ID 040505, 2011.
[25] I. Shimada and T. Nagashima, "A numerical approach to ergodic problem of dissipative dynamical systems," *Progress of Theoretical Physics*, vol. 61, no. 6, pp. 1605–1616, 1979.
[26] W. E. Wiesel, "Continuous time algorithm for Lyapunov exponents," *Physical Review E*, vol. 47, no. 5, pp. 3686–3697, 1993.